JOURNAL OF AGRICULTURAL AND FOOD CHEMISTRY

Chemistry and Phytotoxicity of Thaxtomin A Alkyl Ethers

STUART B. KRASNOFF,*,†,‡ EMIL B. LOBKOVSKY,§ MICHAEL J. WACH,†,|| ROSEMARY LORIA,† AND DONNA M. GIBSON‡

Department of Plant Pathology, Cornell University, Ithaca, New York 14853, Department of Chemistry and Chemical Biology, Ithaca, New York 14853, and USDA-ARS-Plant Protection Research Unit, Ithaca, New York 14853

The thaxtomin phytotoxins (**1** and **2**) from scab-producing *Streptomyces* pathogens of the potato are 2,5-dioxopiperazines consisting of modified L-tryptophanyl and L-phenylalanyl units. Thaxtomin A (**1**) is hydroxylated at C-14, the α carbon of the modified L-phenylalanyl moiety. Refluxing thaxtomin A in acidified MeOH, EtOH, and *i*-PrOH afforded C-14 thaxtomin A methyl- (**3a** and **3b**), ethyl- (**4a** and **4b**), and isopropyl- (**5a** and **5b**) ethers, respectively, in both the 11*S*,14*R* (**3a**, **4a**, and **5a**) and 11*S*,14*S* (**3b**, **4b**, and **5b**) configurations. Crystal structures were determined for **3a** and **4a**. Extensive NMR as well as other spectroscopic data supported structural assignments for all of the derivatives. The 11*S*,14*R*-configured derivatives were slightly less potent than the natural products (**1** and **2**) as inhibitors of lettuce seedling root growth, whereas the activity of the 11*S*,14*S* epimers was much reduced, indicating that the configuration at C-14 found in the naturally occurring thaxtomins is essential for biological activity. Among the 11*S*,14*R*-configured compounds, potency decreased with an increasing size of the substituted alkoxy group.

KEYWORDS: Thaxtomins; crystal structure; phytotoxin; *Streptomyces*

INTRODUCTION

Plant pathogenic *Streptomyces* species, including *S. scabies*, *S. acidiscabies*, and *S. turgidiscabies*, cause scab disease of the potato (*Solanum tuberosum*), which is characterized by conspicuous corky lesions on tubers that diminish marketability. These *Streptomyces* spp. produce the phytotoxic thaxtomins (*1*−*5*) (**Figure 1**), which are required for lesion development on tubers (*6*). Mode-of-action studies indicate that thaxtomin A (**1**) inhibits cellulose biosynthesis (*7*, *8*). A recent study showed that thaxtomin A affects the movement of calcium ions and protons across the plasma membrane, suggesting that these phytotoxins trigger an "early signaling cascade" that may mediate plant−microbe interactions (*9*). Molecular genetic investigations, using a gene-knockout approach, have shown that thaxtomins are biosynthesized by a nonribosomal peptide synthetase that condenses modified L-phenylalanyl and L-4-nitrotryptophanyl units to form a 2,5-dioxopiperazine (*10*). A cytochrome P450 monooxygenase hydroxylates the α carbon and one of the ring carbons of the phenylalanyl moiety (*11*), and a nitric oxide synthase contributes nitric oxide used in the nitration of the trytophanyl unit (*12*). The genes for these biosynthetic enzymes reside on a discrete, mobilizable chromosomal region called a "pathogenicity island", that is common to all scab-producing *Streptomyces* spp. (*13*).

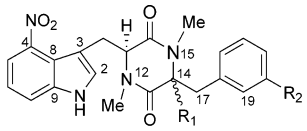

1 R_1 = ····OH R_2 = —OH **2** R_1 = —H R_2 = —H

3a R_1 = ····OMe R_2 = —OH **3b** R_1 = ◄OMe R_2 = —OH

4a R_1 = ····OEt R_2 = —OH **4b** R_1 = ◄OEt R_2 = —OH

5a R_1 = ····Oi-Pr R_2 = —OH **5b** R_1 = ◄Oi-Pr R_2 = —OH

Figure 1. Structures of the natural products thaxtomins A (**1**), D (**2**), and C-14 alkyl ether derivatives with either the 11*S*,14*R* configuration (**3a**, **4a**, and **5a**) or the 11*S*,14*S* configuration (**3b**, **4b**, and **5b**).

The hydroxyl group at C-14 and the position of the hydroxyl group on the phenyl ring of thaxtomin A appear to be critical for its phytotoxicity (*14*). Glucosylation of the C-14 hydroxyl group substantially reduced phytotoxic activity and has been proposed as a possible detoxification mechanism *in planta* (*15*, *16*). During efforts to further explore structure/activity relationships among the thaxtomins, we developed a method for producing C-14-alkoxy derivatives of thaxtomin A (**1**). A small panel of derivatives (**3a**, **3b**, **4a**, **4b**, **5a**, and **5b**) was produced, which then presented an opportunity to study the effect of stereochemistry and the size of the substituent group at C-14 on the phytotoxic activity of the thaxtomins. The chemistry of

* To whom correspondence should be addressed. Telephone: (607) 255-2026. Fax: (607) 255-1132. E-mail: sbk1@cornell.edu.
† Department of Plant Pathology, Cornell University.
‡ USDA-ARS-PPRU.
§ Department of Chemistry and Chemical Biology, Cornell University.
|| Current address: USDA/APHIS/BRS, 6B57, 4700 River Rd., Riverdale, MD 20737.

10.1021/jf051614w CCC: $30.25
Published on Web 11/01/2005

Table 1. NMR Data for **1** and **2** (CD_3OD)

	1					2		
number	δ ^{13}C[a]	δ ^{15}N[b]	δ ^{1}H mult (*J*, Hz)[c]	HMBC[d]	^{15}N-HMBC[e]	δ ^{13}C[f]	δ ^{1}H mult (*J*, Hz)[c]	HMBC[d]
1		132.2						
2	132.4		6.95 s	3, 4, 8, 9, 10, 11	1	132.0	7.09 s	3, 8, 9, 10
3	110.4					110.4		
4	143.6					144.2		
5	118.4		7.84 dd (7.8, 0.9)	3, 4, 6, 7	26	118.8	7.85 dd (7.9, 0.9)	4, 7, 8
6	120.9		7.19 t (7.9)	4, 5, 7, 9	1, 26	121.4	7.23 t (8.0)	4, 5, 9
7	119.1		7.70 dd (8.0, 0.6)	4, 5, 6	1, 26	119.3	7.73 dd (8.1, 1.0)	5, 8
8	119.6					120.1		
9	141.1					141.1		
10	33.5		1.61 dd (14.2, 8.9)	2, 3, 8, 11, 16	12, 15	32.3	2.41 dd (14.6, 7.5)	2, 3, 8, 11, 16
			2.60 dd (14.1, 6.3)	2, 3, 8, 11, 16	12		2.97 m	2, 3, 8, 11, 16
11	64.5		3.86 dd (8.8, 6.4)	3, 10, 13, 16	12, 15	65.3	3.97 dd (7.5, 5.7)	2, 3, 10, 13, 16
12		125.2						
13	168.4					167.90		13, 16, 17, 18
14	88.0					65.5	4.18 dd (5.6, 4.6)	
15		114.6						13, 14, 18
16	166.9					167.5		
17	43.6		3.12 d (13.6)	13, 14, 18, 19, 23	12, 15	39.5	2.62 dd (14.2, 5.7)	
			3.31 d (13.5)	13, 14, 18, 19, 23	15		2.98 m	17, 21, 23
18	137.4					138.3		18, 22
19	118.5		6.70[g] m	17, 18, 20, 23		131.1	7.10 m	18, 19, 23
20	159.1					130.2	7.36 m	18, 20
21	115.8		6.75 ddd (8.1, 2.4, 1.0)	19, 20, 23		128.6	7.27 m	17, 19, 21
22	131.1		7.23 t (8.0)	17, 18, 19, 20, 21, 23		130.2	7.36 m	11, 13
23	122.7		6.70[g] m	17, 18, 19, 22		131.2	7.10 m	14, 16
24 (N-12-CH_3)	34.1		2.82 s	11, 13	12	33.9	2.86 s	
25 (N-15-CH_3)	28.3		3.03 s	14, 16	15	33.7	2.76 s	
NO_2		374.8						

[a] Resonances from HMQC, HMBC spectra. [b] 40.5 MHz (reported in ref *12*). [c] 500 MHz. [d] Numbers indicate carbons showing long-range correlations with the proton at the position designated in column 1. [e] Numbers indicate nitrogens showing long-range correlations with the proton at the position designated in column 1. [f] 100 MHZ. [g] HMQC spectrum showed H-19 downfield of H-23.

these derivatives and the results of this phytotoxicity study are reported herein.

MATERIALS AND METHODS

Polarimetry. Optical rotations were measured at 25 °C in MeOH on a Perkin−Elmer 241 polarimeter using the sodium lamp (589 nm) with a 100 mm cell.

Analytical HPLC. HPLC retention times were determined on a 250 × 4.6 mm, 5 μm, 100 Å, RPC18Prodigy ODS(3) column (Phenomenex) using a premixed isocratic mobile phase [2:3, AcN/H_2O (v/v)] at a flow rate of 1 mL/min with detection by absorption at 225 and 380 nm.

Electrospray Mass Spectrometry. Low-resolution ESI mass spectra were acquired by infusion of methanolic solutions at 5 μL/min via a syringe pump (Harvard Apparatus) into a Micromass ZMD 4000 spectrometer. Positive-ion-mode spectra were taken with capillary and cone voltages of 3.4 kV and 50 V, respectively; negative-ion-mode spectra were taken with capillary and cone voltages of 3.4 kV and 50 V, respectively. High-resolution ESI mass spectra were acquired on a Micromass QTOF Ultima instrument with capillary and cone voltages of 3 kV and 35 V, respectively.

UV−Vis Spectrometry. UV spectra were obtained in MeOH on a Beckmann DU 640 spectrophotometer.

NMR Spectroscopy. ^{1}H NMR spectra were acquired on Varian Mercury 300 or Inova 400, 500, and 600 spectrometers. ^{13}C NMR spectra were acquired at 125 MHz. HMQC (HSQC for **3b**) and HMBC spectra were acquired at 600 or 500 MHz (^{1}H dimension), and experiments were optimized for $^{1}J_{CH} = 150$ Hz and $^{n}J_{CH} = 5.0$ (and 8.0 Hz for **1**, **3b**, and **5b**), respectively. COSY spectra were acquired at 400, 500, or 600 MHz. All NMR data were recorded in CD_3OD, and chemical shifts were referenced to the centers of the residual CHD_2-OD quintuplet at δ 3.31 and the $^{13}CD_3OD$ septuplet at δ_C 49.15.

X-ray Diffraction. Crystals (orange-yellow prisms) were transferred to a microscope slide in a drop of polybutenes oil. Using a nylon loop, a suitable single crystal was picked and mounted on a Bruker 1K CCD diffractometer (Mo radiation) and cooled to −100 °C. Data collection and reduction were performed using Bruker SMART and SAINT software packages. For **3a**, the crystal dimensions were 0.30 × 0.20 × 0.20 mm. Overall, 7248 reflections were collected, and 3916 reflections were symmetry-independent ($R_{int} = 0.0216$), with 3494 "strong" reflections ($F_o > 4\sigma F_o$). For **4a**, the crystal dimensions were 0.20 × 0.10 × 0.02 mm. Overall, 6734 reflections were collected, and 2626 reflections were symmetry-independent ($R_{int} = 0.075$), with 2048 "strong" reflections. Both structures were solved by a direct method and subsequent difference Fourier techniques (SHELXTL). All non-hydrogen atoms were refined anisotropically. Hydrogen atoms were found in a difference Fourier map and refined isotropically. **4a** cocrystallized with half of a water molecule per asymmetric unit, while **3a** cocrystallized with one methanol molecule per asymmetric unit. Final $R_1 = 0.0350$ and 0.0652 for the **3a** and **4a** structures, respectively.

Lettuce Seedling Root Growth Inhibition Bioassay. Solutions were applied in 0.5 mL of MeOH to the bottom of 50 mm Petri plates. After solvent evaporation (15 min), 2.0 mL of 1.6% agarose was pipetted into each plate, agitated briefly by hand, and set to cool for 1 h at 22 °C. Thus, the original concentration of MeOH solutions was reduced by a factor of 4 in the agar. Lettuce seeds (*Lactuca sativa* cv. black-seeded Simpson) were located in a row of 10 on the surface of each plate ca. 20 mm from the "top" edge of the plate at the center of the row with the root ends all pointed in the same direction. Plates were covered, sealed with Parafilm, and stored upright (with root ends pointed down) in a darkened growth chamber at 22 °C. Root lengths were measured at 96 h.

Two plates of 10 seeds each were set up for each dosage of each compound. Measurements were averaged for 20 measurements/point, and percent inhibition relative to the mean growth response in MeOH-treated control plates was calculated. Dose−response curves were fit to a four-parameter logistic model (*17*), and I_{50} values were estimated from these curves.

Fermentation, Extraction, and Isolation. Thaxtomins A and D were extracted and purified from fermentation broths of *Streptomyces scabies*, *S. acidiscabies*, and *S. turgidiscabies* as described previously

Table 2. NMR Data for **3a** and **3b** (CD_3OD)

	3a			3b		
number	δ ^{13}C[a]	δ ^{1}H mult (*J*, Hz)[b]	HMBC[c]	δ ^{13}C[a]	δ ^{1}H mult (*J*, Hz)[b]	HMBC[c]
2	132.7	6.94 s	3, 4, 8, 9, 10, 11	131.0	7.25 s	3, 4, 8, 9, 10
3	110.5			108.6		
4	143.7			144.7		
5	118.6	7.85 dd (7.9, 0.9)	3, 4, 6, 7	118.8	7.75 (dd 7.8, 0.9)	3, 4, 6, 7
6	121.2	7.20 t (8.0)	4, 5, 7, 9	121.4	7.19 (t 7.9)	4, 5, 7, 9
7	119.5	7.70 dd (8.1, 0.9)	4, 5, 6	118.6	7.64 dd (8.1, 0.9)	4, 5, 6
8	119.9			120.3		
9	141.3			140.7		
10	33.8	1.58 dd (14.1, 8.9)	2, 3, 8, 11, 16	29.5	3.32 dd (15.3, 4.3)[d]	2, 3, 8, 11, 16
		2.62 dd, (14.0, 6.2)	2, 3, 8, 11, 16		3.66 dd (15.3, 3.6)	2, 3, 8, 11, 16
11	64.6	3.96 dd, (8.9, 6.3)	3, 10, 13, 16, 24	63.6	3.17 t (3.9)	3, 10, 13, 16, 24
13	165.7			166.2		
14	93.8			93.3		
16	167.9			168.4		
17	43.1	3.13 d (13.6)	13, 14, 18, 19, 23	44.3	2.86 d (13.4)	13, 14, 18, 19, 23
		3.29 d (13.8)	13, 14, 18, 19, 23		2.89 d (13.5)	13, 14, 18, 19, 23
18	137.0			135.9		
19	118.9	6.72 m	17, 20, 23	117.8	6.38 m	17, 20, 23
20	159.3			158.8		
21	116.2	6.76 ddd (8.1, 2.4, 1.0)	19, 20, 23	116.0	6.68 ddd (8.2, 2.5, 0.9)	19, 23
22	131.4	7.24 (t, 8.1)	18, 19, 20, 21, 23	130.7	7.06 t (7.8)	18, 19, 20
23	123.0	6.71 m	17, 22	121.9	6.37 m	17, 19, 21
24 (N-12-CH_3)	34.2	2.85 s	11, 13	33.4	2.84 s	11, 13
25 (N-15-CH_3)	28.1	2.99 s	14, 16	27.5	2.61 s	14, 16
26 (OCH_3)	51.4	3.03 s	14	50.8	1.95 s	14

[a] 125 MHz. [b] 500 MHz. [c] Numbers indicate carbons showing long-range correlations with the proton at the position designated in column 1. [d] Multiplicity and ^2J coupling constant inferred from the geminal proton because of partial signal overlap with the solvent signal.

Table 3. NMR Data for **4a** and **4b** (CD_3OD)[a]

	4a			4b		
number	δ ^{13}C[b]	δ ^{1}H mult (*J*, Hz)[c]	HMBC[d]	δ ^{13}C[b]	δ ^{1}H mult (*J*, Hz)[c]	HMBC[d]
24 (N-12-CH_3)	34.2	2.84 s	11, 13	33.4	2.83 s	11, 13
25 (N-15-CH_3)	28.2	2.99 s	14, 16	27.6	2.60 s	14, 16
26 (O*CH*$_2$-CH_3)	60.2	3.15 m	14, 27	59.5	1.33 dq (8.8, 7.1)	14, 27
					2.00 dq (8.8, 7.0)	14, 27
27 (OCH_2-*CH*$_3$)	15.2	1.18 t (7.0)	26	14.8	0.76 t (7.0)	26

[a] Data are presented for atoms in **4a** and **4b** for which resonances differed substantially from those for corresponding atoms in **3a** and **3b**. See the Supporting Information for a complete table. [b] 125 MHz. [c] 500 MHz. [d] Numbers indicate carbons showing long-range correlations with the proton at the position designated in column 1.

(*11*). Briefly, *Streptomyces* strains were grown in oatmeal broth in 100 mL batches. After the development of a yellow color (3−5 days), the broth was filtered and extracted with ethyl acetate. Thaxtomins were purified from the dried extract by flash chromatography on silica gel using dichloromethane/MeOH mixtures and crystallization by slow evaporation from MeOH.

Compound 1. Orange-yellow crystals (rosettes of fine needles) (MeOH). $[\alpha]^{25}_D$ +166.3 (*c* 0.0024, MeOH). HPLC t_R, 5.59 min. ESI−MS *m/z* $[M + Na]^+$, 461; $[M - H]^-$, 437. UV (MeOH) λ_{max} (ϵ), 227 (12 500), 255 (7300), 280 (3100) 355 (2800), and 394 (3300) nm. ^{1}H NMR, ^{13}C NMR, and HMBC data, see **Table 1**.

Compound 2. Lemon-yellow crystals (rosettes of fine needles) (MeOH). $[\alpha]^{25}_D$ +56 (*c* 0.0026, MeOH). HPLC t_R, 12.36 min. ESI−MS *m/z* $[M + Na]^+$, 429; $[M - H]^-$, 405. UV (MeOH) λ_{max} (ϵ), 224 (12 500), 249 (7800), 280 (2600) 354 (2400), and 396 (3000) nm. ^{1}H NMR, ^{13}C NMR, and HMBC data, see **Table 1**.

Thaxtomin Ether Derivitization. Thaxtomin A (**1**) (5.0 mg) was dissolved in 50 mL of MeOH/0.1% TFA and refluxed for 17 h. The reaction mixture was dried in vacuo, reconstituted in 1 mL of MeOH, and fractionated by semipreparative HPLC on a IB-Sil RPC18, 5 μm, 120 Å column (Phenomenex) in AcN/H_2O (9:11, v/v) at a flow rate of 4 mL/min with detection by UV absorption at 225 and 380 nm. After removal of the solvent in vacuo, two major fractions afforded **3a** (2.0 mg) and **3b** (2.8 mg).

Compound 3a. Orange-yellow prisms (MeOH). $[\alpha]^{25}_D$ +163 (*c* 0.0023, MeOH). HPLC t_R, 8.87 min. HRESI−MS *m/z* $[M + H]^+$, 453.1751 (calcd for $C_{23}H_{25}N_4O_6$, 453.1774]. UV (MeOH) λ_{max} (ϵ), 225 (13 100), 248 (10 300), 280 (4300) 351 (3200), and 394 (3800) nm. ^{1}H NMR, ^{13}C NMR, and HMBC data, see **Table 2**.

Compound 3b. Brownish-yellow oil. $[\alpha]^{25}_D$ +113 (*c* 0.0014, MeOH). HPLC t_R, 7.58 min. HRESI−MS *m/z* $[M + H]^+$, 453.1772 (calcd for $C_{23}H_{25}N_4O_6$, 453.1774]. UV (MeOH) λ_{max} (ϵ), (MeOH) 218 (16 900), 248 (5600), 280 (2700) 337 (2400), and 375 (2600) nm. ^{1}H NMR, ^{13}C NMR, and HMBC data, see **Table 2**.

Thaxtomin A (**1**) (12.5 mg) was dissolved in 100 mL of EtOH/0.1% TFA and refluxed for 17 h. The reaction mixture was dried in vacuo, reconstituted in 1 mL of EtOH, and fractionated by HPLC as for **3a** and **3b**. After removal of the solvent in vacuo, two major fractions afforded **4a** (5.4 mg) and **4b** (5.4 mg).

Compound 4a. Orange-yellow crystals (MeOH). $[\alpha]^{25}_D$ +157 (*c* 0.0033, MeOH). HPLC t_R, 12.12 min. HRESI−MS *m/z* $[M + H]^+$, 467.1941 (calcd for $C_{24}H_{27}N_4O_6$, 467.1931). UV (MeOH) λ_{max} (ϵ), 222 (17 100), 252 (6000), 275 (2700) 350 (2000), and 397 (2400) nm. ^{1}H NMR, ^{13}C NMR, and HMBC data, see **Table 3**.

Compound 4b. Brownish-yellow oil. $[\alpha]^{25}_D$ +203 (*c* 0.003, MeOH). HPLC t_R, 9.19 min. HRESI−MS *m/z* $[M + H]^+$, 467.1917 (calcd for $C_{24}H_{27}N_4O_6$, 467.1931). UV (MeOH) λ_{max} (ϵ), 219 (11 200), 235 (7000), 247 (5100), 277 (2300), 341 (2500), and 376 (2800) nm. ^{1}H NMR, ^{13}C NMR, and HMBC data, see **Table 3**.

Thaxtomin A (**1**) (15.4 mg) was dissolved in 100 mL of *i*-PrOH/0.1% TFA and refluxed for 24 h. The reaction mixture was dried in

Table 4. NMR Data for **5a** and **5b**[a]

	5a			5b		
number	δ ^{13}C[b]	δ ^{1}H mult (*J*, Hz)[c]	HMBC[d]	δ ^{13}C[b]	δ ^{1}H mult (*J*, Hz)[c]	HMBC[d]
24 (N-12-CH_3)	34.4	2.85 s	11, 13	33.6	2.83 s	11, 13
25 (N-15-CH_3)	29.6	3.02 s	14, 16	29.7	2.73 s	14, 16
26 (O*CH*-$(CH_3)_2$	69.5	3.61 sept (6.1)	14, 27, 28	69.8	1.93 sept (6.1)	14, 27, 28
27 (OCH-(CH_3)$_2$a	23.8	1.09 d (6.2)	26, 28	23.5	0.37 d (6.1)	26, 28
28 (OCH-(CH_3)$_2$b	23.6	1.11 d (6.1)	26, 27	23.6	0.71 d (6.1)	26, 27

[a] Data are presented for atoms in **5a** and **5b** for which resonances differed substantially from those for corresponding atoms in **3a** and **3b**. See the Supporting Information for a complete table. [b] 125 MHz. [c] 500 MHz. [d] Numbers indicate carbons showing long-range correlations with the proton at the position designated in column 1.

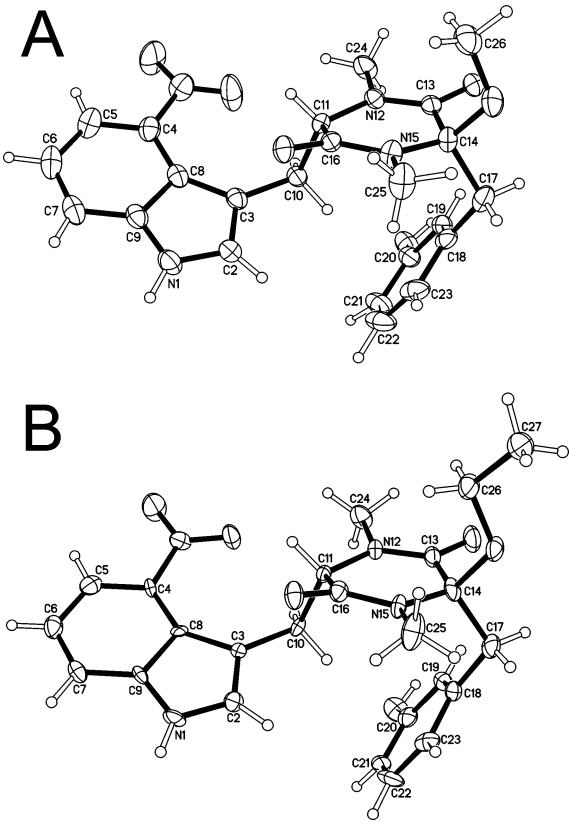

Figure 2. ORTEP view of **3a** (A) and **4a** (B) (solvent molecules omitted). Ellipsoids are represented with 40% probability.

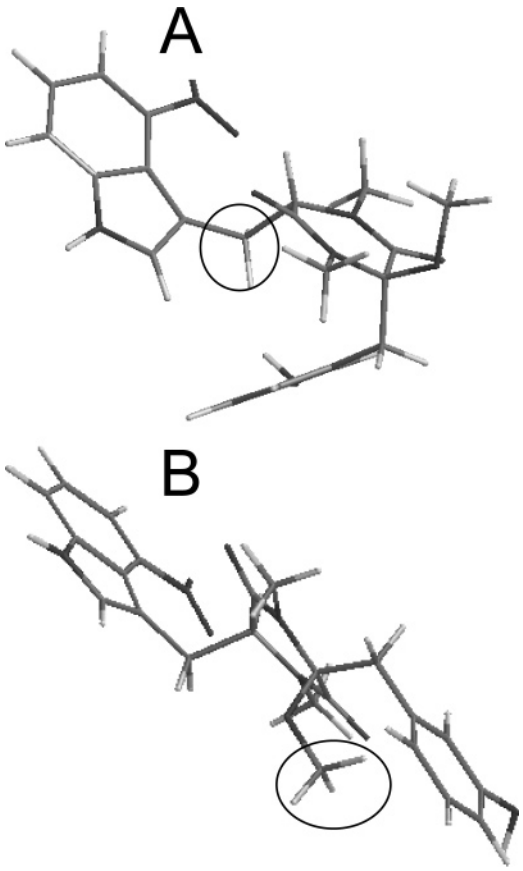

Figure 3. (A) Perspective of the crystal structure of **3a**. (B) Model of **3b** constructed by reversing the chirality at C-14 of the model of **3a** while preserving all bond lengths and angles. The upfield NMR chemical shifts of the circled protons (the C10 protons in **A** and the *O*-Me protons in **B**) (see Table 2) are consistent with the proximity and disposition of these protons to the phenyl ring of the hydroxyphenylalanyl moiety and the shielding effect of a ring current.

vacuo, reconstituted in 1 mL of *i*-PrOH, and fractionated by HPLC as for **3a** and **3b**, except that a mobile phase of AcN/H_2O (1:1) was used. After removal of the solvent in vacuo, two major fractions afforded **5a** (5.2 mg) and **5b** (4.4 mg).

Compound 5a. Yellow oil. $[\alpha]^{25}_D$ +188 (*c* 0.0022, MeOH). HPLC t_R, 18.17 min. HRESI−MS *m*/*z* $[M + H]^+$, 481.2083 (calcd for $C_{25}H_{29}N_4O_6$, 481.2087). UV (MeOH) λ_{max} (ϵ), 224 (17 800), 255 (6800), 279 (2800), 358 (2400), and 397 (2900) nm. ^{1}H NMR, ^{13}C NMR, and HMBC data, see **Table 4**.

Compound 5b. Brownish-yellow oil. $[\alpha]^{25}_D$ +0 (*c* 0.0027, MeOH). HPLC t_R, 11.89 min. HRESI−MS *m*/*z* $[M + H]^+$, 481.2076 (calcd for $C_{25}H_{29}N_4O_6$, 481.2087). UV (MeOH) λ_{max} (ϵ), 220 (16 000), 273 (3500), 338 (2600), and 375 (2800) nm. ^{1}H NMR, ^{13}C NMR, and HMBC data, see **Table 4**.

RESULTS AND DISCUSSION

Refluxing thaxtomin A (**1**) in MeOH yielded a mixture of two yellow compounds in a ratio of ca. 2:3 with RP-HPLC retention times of 5.5 and 6.1 min, respectively. After HPLC purification, ESI−mass spectrometry indicated a molecular weight of 452 Da for both products. The more abundant later-eluting compound crystallized after slow evaporation from MeOH. Single-crystal X-ray diffraction data were consistent with compound **3a** or its enantiomer (**Figure 2A**; see the Supporting Information). The crystal structure of **3a** is very similar to a published crystal structure of **1** (*18*).

The absolute configuration of compound **3a** (**Figures 1** and **2A**) was deduced as 11*S*,14*R* from that of its precursor (**1**) (*2*, *18*) based on the assumption that the *S* configuration at C-11 in the natural product remained unaltered by the reaction. One- and two-dimensional NMR data supported this inference (**Figures 1** and **2B**). The *O*-methyl proton resonances were observed at δ 3.03 in **3a** and δ 1.95 in **3b**. Concomitantly, the signals of the diastereotopic C-10 methylene protons appeared at δ 1.58 and 2.62 in **3a** (the 11*S*,14*R* epimer) and at δ 3.32 and 3.66 in **3b** (the 11*S*,14*S* epimer). These observations can

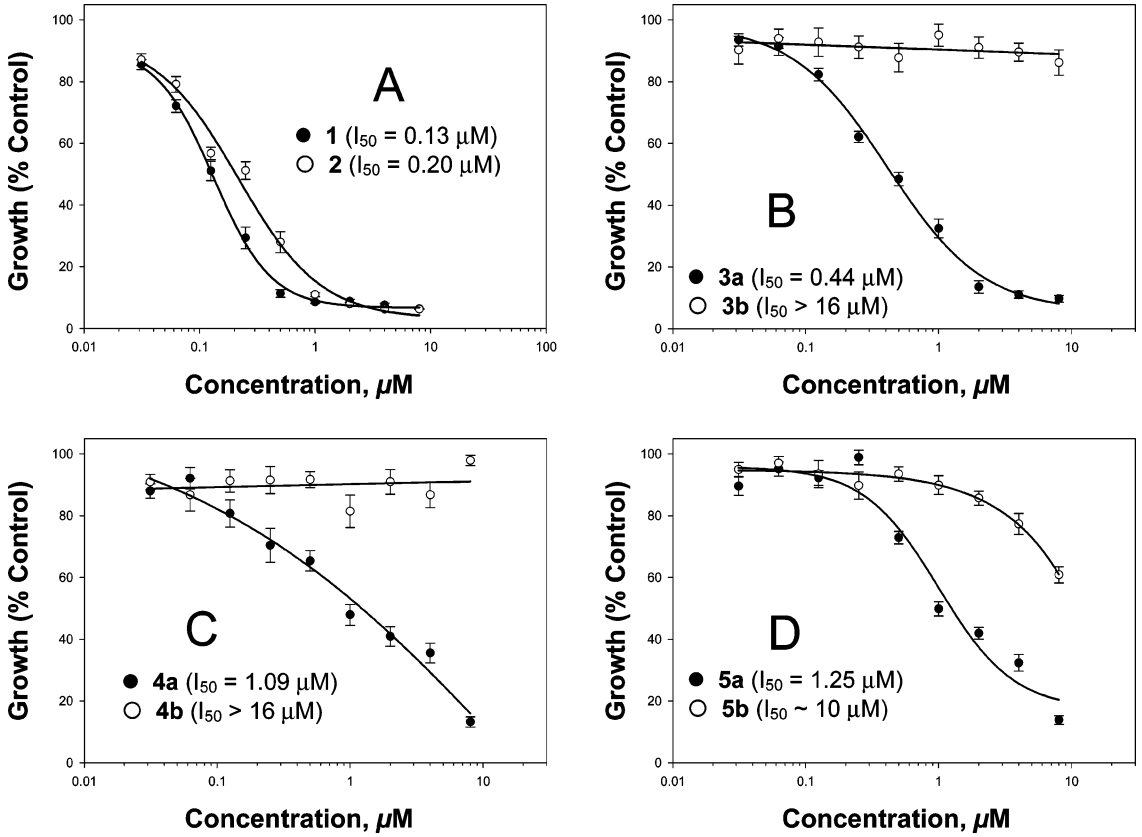

Figure 4. Inhibition of lettuce seedling growth on water agar plates by **1** and **2** (A), **3a** and **3b** (B), **4a** and **4b** (C), and **5a** and **5b** (D). Each point represents the mean (±SEM) of 20 measurements.

be explained by the shielding effect of the phenylalanyl ring current and the difference in proximity to the ring of the *O*-methyl and C-10 protons in the two epimers (parts **A** and **B** of **Figure 3**). Unusual upfield shifts induced by a ring current have been observed for similarly disposed *O*-methyl protons in diastereomeric diketopiperazines (*19*).

In a fashion analogous to the production of **3a** and **3b**, refluxing compound **1** in EtOH and *i*-PrOH yielded diastereomeric pairs of the C-14-ethoxy (**4a** and **4b**) and isopropoxy (**5a** and **5b**) derivatives of **1**. The crystal structure obtained for compound **4a** was very similar to that of compound **3a** (**Figure 2B**; see the Supporting Information), and thus the absolute configurations of **4a** and **4b** were assigned by analogy to **3a** and **3b**. The absolute configurations of **5a** and **5b** were assigned as 11*S*,14*R* and 11*S*,14*S*, respectively, on the basis of the downfield NMR signals of the protons in the isopropyl group of **5a** and the upfield resonances of the corresponding protons in **5b** (**Table 4**).

Except for predictable differences because of the substituent groups on C-14, ^{13}C and ^{1}H NMR assignments were virtually identical for all carbons and protons for like-configured derivatives (**Tables 2**−**4**). Except for the protons and carbon atoms of the alkoxy groups, the assignments for the 11*S*,14*R* epimers were virtually identical to those of the precursor, compound **1** (**Table 1**).

Compounds **3a**, **3b**, **4b**, **5a**, and **5b** are previously unreported. Compound **4a** was previously reported as a biotransformant of thaxtomin A (**1**) by *Aspergillus niger* (*20*). In the published procedure, thaxtomin A (**1**) was introduced as an ethanolic solution into the fungal growth medium, in which, it was noted, the pH rapidly dropped below 2.0 by the second day of fermentation, at which point **4a** was detected. We suggest that under these conditions **4a** may be produced nonenzymatically as a consequence of the low pH of the fungal culture medium and the presence of EtOH as the donor of the ethoxy group.

The N-15-methyl proton signals of the 11*S*,14*S*-configured diastereomers were upfield of the N-12-methyl proton resonances in the 11*S*,14*S*-configured diastereomers but downfield in the 11*S*,14*R* compounds. In a prior study (*2*), N-15-methyl signals were observed upfield of the N-12 signals in **1**, which is also 11*S*,14*R*-configured. This apparent inconsistency with our NMR data for the 11*S*,14*R*-configured alkyl ether derivatives led us to re-examine the assignments of **1**. Data from ^{1}H-^{13}C and ^{1}H-^{15}N HMBC experiments support the assignments presented in **Table 1**, which are consistent with another set of assignments based on spectra obtained for **1** in $(CD_3)_2SO$ (*18*). The ^{13}C NMR assignments for **2** have not been reported previously (**Table 1**).

Phytotoxicity Bioassay—Structure—Activity Relationship. On the basis of the I_{50} values derived from a lettuce seedling root elongation assay, the order of plant growth inhibiting activity among the compounds tested was **1** > **2** > **3a** > **4a** > **5a** ≫ **5b** > **3b** > **4b**. The reduced potency of **2** relative to **1** supports the view that the hydroxyl groups contribute to the activity of thaxtomin A, but their absence does not abolish activity entirely.

None of the derivatives were as active as either of the natural products (**1** and **2**), although the 11*S*,14*R*-configured diastereomers all showed inhibitory activity in the dosage-range tested, with compound **3a** exhibiting an I_{50} of 440 nM, which was approximately one-third the potency of thaxtomin A (**1**) (**Figure 4**). Among the 11*S*,14*S*-configured epimers, only the isopropoxy compound exhibited any detectable effect. This indicates that the configuration at C-14 seen in the naturally occurring thaxtomins is essential for their biological activity. Among the 11*S*,14*R* epimers, activity decreased as the size of the substitu-

tion at C-14 increased. Thus, it is apparent that the addition of alkoxy groups of greater size would not be a promising route to pursue for increasing the herbicidal activity of the natural product. The weak but detectable activity of **5b** but not of **3b** and **4b** suggests that the activity of the 11*S*,14*S* epimers may increase with the size of the group substituted at C-14. This remains speculative in the absence of more data points from analogues with larger substituents.

ACKNOWLEDGMENT

We gratefully acknowledge Ivan Keresztes and Anthony Condo, Jr. (Cornell University) for help in acquiring NMR spectra and the Mass Spectrometry facility at the University of Illinois, Urbana, for acquiring HRESI−MS data. We also thank L. A. Henderson, J. D. Leehr, W. T. Lester, and J. E. Williams for technical assistance.

Supporting Information Available: Crystallographic data, CIF files for **3a** and **4a**, and complete NMR assignment tables for **4a**, **4b**, **5a**, and **5b**. This material is available free of charge via the Internet at http://pubs.acs.org.

LITERATURE CITED

(1) King, R. R.; Lawrence, C. H.; Clark, M. C.; Calhoun, L. A. Isolation and characterization of phytotoxins associated with *Streptomyces scabies*. *J. Chem. Soc., Chem. Commun.* **1989**, *13*, 849−850.

(2) King, R. R.; Lawrence, C. H.; Calhoun, L. A. Chemistry of phytotoxins associated with *Streptomyces* scabies, the causal organism of potato common scab. *J. Agric. Food Chem.* **1992**, *40*, 834−837.

(3) King, R., R.; Lawrence, C. H. Characterization of new thaxtomin A analogues generated *in vitro* by *Streptomyces scabies*. *J. Agric. Food Chem.* **1996**, *44*, 1108−1110.

(4) King, R. R.; Lawrence, C. H.; Calhoun, L. A.; Ristaino, J. B. Isolation and characterization of thaxtomin-type phytotoxins associated with *Streptomyces ipomoeae*. *J. Agric. Food Chem.* **1994**, *42*, 1791−1794.

(5) King, R. R.; Lawrence, C. H.; Embletona, J.; Calhoun, L. A. More chemistry of the thaxtomin phytotoxins. *Phytochemistry* **2003**, *64*, 1091−1096.

(6) Lawrence, C. H.; Clark, M. C.; King, R. R. Induction of common scab symptoms in aseptically cultured potato tubers by the vivotoxin thaxtomin. *Phytopathology* **1990**, *80*, 606−608.

(7) Fry, B. A.; Loria, R. Thaxtomin A: Evidence for a plant cell wall target. *Physiol. Mol. Plant Pathol.* **2002**, *60*, 1−8.

(8) Scheible, W.-R.; Fry, B.; Kochevenko, A.; Schindelasch, D.; Zimmerli, L.; Somerville, S.; Loria, R.; Somerville, C. R. An *Arabidopsis* mutant resistant to thaxtomin A, a cellulose synthesis inhibitor from *Streptomyces* species. *Plant Cell* **2003**, *15*, 1781−1794.

(9) Tegg, R. S.; Melian, L.; Wilson, C. R.; Shabala, S. Plant cell growth and ion flux responses to the streptomycete phytotoxin thaxtomin A: Calcium and hydrogen flux patterns revealed by the non-invasive MIFE technique. *Plant Cell Physiol.* **2005**, *46*, 638−648.

(10) Healy, F.; Wach, M.; Krasnoff, S. B.; Gibson, D. M.; Loria, R. The txtAB genes of the plant pathogen *Streptomyces acidiscabies* encode a peptide synthetase required for phytotoxin thaxtomin A production and pathogenicity. *Mol. Microbiol.* **2000**, *38*, 794−804.

(11) Healy, F.; Krasnoff, S. B.; Wach, M.; Gibson, D. M.; Loria, R. Involvement of a cytochrome P450 monooxygenase in thaxtomin A biosynthesis by *Streptomyces acidiscabies*. *J. Bacteriol.* **2002**, *184*, 2019−2029.

(12) Kers, J. A.; Wach, M. J.; Krasnoff, S. B.; Widom, J.; Cameron, K. D.; Bukhalid, R. A.; Gibson, D. M.; Crane, B. R.; Loria, R. Nitration of a peptide phytotoxin by bacterial nitric oxide synthase. *Nature* **2004**, *2504*, 1−5.

(13) Kers, J. A.; Cameron, K. D.; Joshi, M. V..; Bukhalid, R. A.; Morello, J. E.; Wach, M. J.; D. M. Gibson, D. M.; Loria, R. A large, mobile pathogenicity island confers plant pathogenicity on *Streptomyces* species. *Mol. Microbiol.* **2005**, *55*, 1025−1033.

(14) King, R. R.; Lawrence, C. H. Herbicidal properties of the thaxtomin group of phytotoxins. *J. Agric. Food Chem.* **2001**, *49*, 2298−2301.

(15) King, R. R.; Lawrence, C. H. Microbial glucosylation of thaxtomin A, a partial detoxification. *J. Agric. Food Chem.* **2000**, *48*, 512−514.

(16) Acuña, I. A.; Strobel, G. A.; Jacobsen, B. J.; Corsini, D. L. Glucosylation as a mechanism of resistance to thaxtomin A in potatoes. *Plant Sci.* **2001**, *161*, 77−88.

(17) Streibig, J. C.; Rudemo, M.; Jensen, J. E. Dose−response curves and statistical models. In *Herbicide Bioassays*; Streibig, J. C., Kudsk, P., Eds.; CRC Press: Boca Raton, FL, 1993; pp 29−55.

(18) Wagner, O. *Sekundärstoffbildende Actinomyceten aus der Umgebung Göttingens: Isolierung, Strukturaufklärung und Biosynthese ausgewählter Metabolite*; University of Göttingen: Göttingen, Germany, 2000.

(19) Marcuccio, S. M.; Elix, J. A. Pyrazine chemistry. V: Synthesis of methylanhydropicroroccellin and dimethylpicroroccellin. *Aust. J. Chem.* **1985**, *38*, 1785−1796.

(20) Lazarovits, G.; Hill, J.; King, R. R.; Calhoun, L. A. Biotransformation of the *Streptomyces scabies* phytotoxin thaxtomin A by the fungus *Aspergillus niger*. *Can. J. Microbiol.* **2004**, *50*, 121−126.

Received for review July 6, 2005. Revised manuscript received September 21, 2005. Accepted September 21, 2005.

JF051614W